Vrublevsky A. V., Petlin K. A., Kozlov B. N., Chernykh Yu. N., Shnayder O. L.
Research Institute of Cardiology, Tomsk National Research
Medical Center of the Russian Academy of Sciences, Tomsk, Russia

Disturbances of the Thoracic Aorta Biomechanics in Degenerative Aortic Valve Stenosis

Aim	To analyze the biomechanics of the thoracic aorta (TA) in degenerative calcific aortic stenosis (AS) using segmental ultrasound assessment of the aortic wall deformation.
Material and methods	A total of 109 patients with severe AS and 11 healthy volunteers were evaluated. 2D speckle-tracking transesophageal echocardiography was performed in all patients. We calculated the global peak systolic circumferential strain (GCS, %), GCS normalized to pulse arterial pressure (GCS/PAP), and β_2 stiffness index (SI) of the aortic wall at 4 levels of the TA: sinuses of Valsalva (SV), sinotubular junction (STJ), mid-ascending aorta (AA), and descending aorta (DA).
Results	n patients with aortic stenosis, GCS and GCS/PAP in all TA segments were statistically significantly lower than in healthy volunteers (SV: 3.1 [1.3; 4.4] and 3.8 [1.5; 5.9]; 12.2 [9.9; 13.4] and 20.2 [17; 28.6], p<0.001; at STJ level: 4.5 [2.4; 6.5] and 5.7 [3.3; 8.7]; 8.4 [5.6; 10] and 14.7 [10.9; 18.6], p<0.001; at AA level: 3.1 [0.8; 4.7] and 3.9 [1.4; 6.4]; 8.6 [7.6; 11.7] and 18.0 [12.1; 20.2], p<0.001; DA: 3.9 [3.1; 6] and 5.6 [3.6; 8.4]; 10.4 [7; 11.2] and 17.2 [14.1; 21.5], p<0.001, respectively). Furthermore, the SI in AS patients was statistically significantly increased to 19.1 [12.9; 26.5] and 4.8 [3.6; 5.3], p<0.001 in SV; 13.4 [10.1; 19.9] and 6.7 [5.6; 8.3], p<0.001 at STJ level; 17.8 [13.4; 26.9] and 5.6 [4.6; 8.1], p<0.001 at AA; 17.2 [11.1; 25.3] and 5.6 [4.6; 7.4], p<0.001 at DA, respectively. 69 (63.3%) AS patients had multidirectional GCS of the aortic wall in the aortic root and the TA ascending and descending sections. Patients with AS showed a uniform decrease in GCS and GCS/PAD and an increase in the SI and diameters in all TA segments from the aortic annulus to the descending section. In all AA segments, GCS, GCS/PAD and SI did not differ between AS patients with bicuspid aortic valve (AV) (n=47) and tricuspid AV (n=62) (p>0.05). An inverse correlation was found between the mean transaortic pressure gradient and GCS and GCS/PAD in the SV (r=-0.33; p<0.01, and r=-0.26; p<0.01, respectively) and in the AA (r=-0.23; p<0.05 and r=–0.21; p<0.05, respectively).
Conclusion	Severe AS is associated with non-adaptive remodeling of the TA, reduced and multidirectional deformation along the circumference of the aortic wall in the aortic root, and the TA ascending and descending segments, which is closely related to disorders of transaortic hemodynamics.

Keywords	Degenerative calcific aortic stenosis; thoracic aorta; 2D speckle-tracking transesophageal echocardiography; global circumferential strain
For citations	Vrublevsky A.V., Petlin K.A., Kozlov B.N., Tchernykh Yu.N., Schnaider O.L. Disturbances of the Thoracic Aorta Biomechanics in Degenerative Aortic Valve Stenosis. Kardiologiia. 2025;65(7):37–45. [Russian: Врублевский А.В., Петлин К.А., Козлов Б.Н., Черных Ю.Н., Шнайдер О.Л. Нарушения биомеханики грудного отдела аорты при дегенеративном стенозе аортального клапана. Кардиология. 2025;65(7):37–45].
Corresponding author	Vrublevsky Aleksandr Vasilievich. E-mail: avr@cardio-tomsk.ru

Introduction

Degenerative calcific aortic stenosis (AS) is the most common valvular heart disease in developed countries, occurring in 1-2% of individuals aged >65 years and in 12% of individuals aged >75 years [1-3]. Annual mortality from AS worldwide is approximately 125,000 people [1]. The only effective treatment for AS is surgical or transcatheter aortic valve (AV) replacement, with approximately 350,000 such surgeries performed annually [1, 4-6]. Given the close relationship between aging and the incidence of AS, the prevalence of AS is expected to double in the coming decades as life expectancy increases [1].

In recent years, tomographic studies of the AV and thoracic aorta (TA) with the 4D Flow option and analysis of additional blood flow characteristics have indicated that a marked increase in the transaortic pressure gradient in severe AS of both bicuspid and tricuspid AVs leads to a change in the structure and geometry of blood flow in the ascending aorta causing maladaptive remodeling of the aortic wall as a result of disturbances in its biomechanics and the development of one of the aortopathy phenotypes: dilation, aneurysm or dissection [7-12]. These studies undoubtedly expand the capabilities of the algorithm for comprehensive preoperative diagnostics of AV dysfunction and the degree of TA re-

Central illustration. Disorders of the thoracic aorta biomechanics in degenerative stenosis of the aortic valve

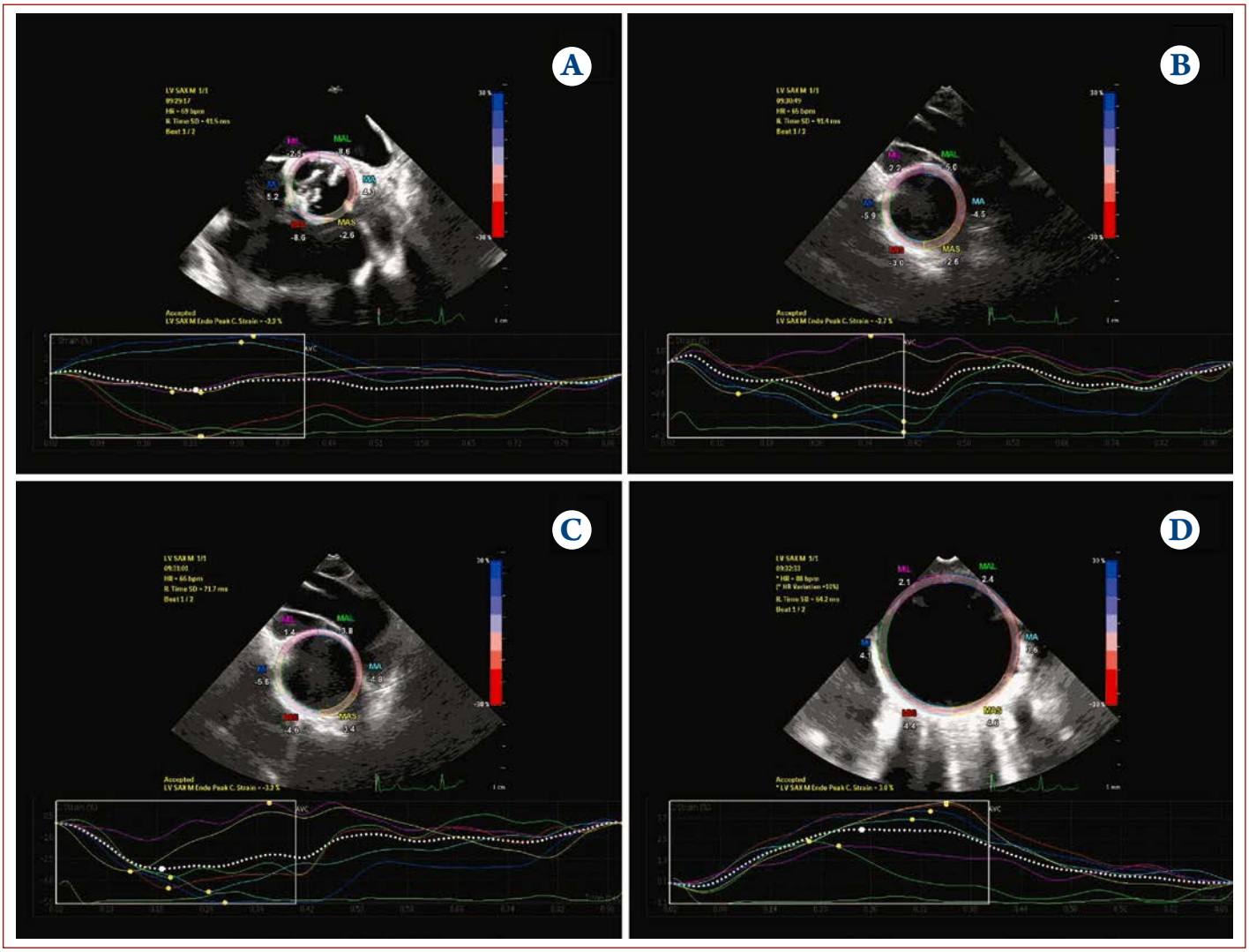

An example of segmental analysis of the aortic wall global circumferential strain in patient I., 61 years old, with bicuspid aortic valve stenosis using 2D speckle-tracking transesophageal echocardiography. A, sinuses of Valsalva: diameter 31 mm, GCS=-2.2%; B, sinotubular junction: diameter 30 mm, GCS=-2.7%; C, ascending aorta (level of pulmonary artery bifurcation): diameter 36 mm, GCS=-3.2%; D, proximal segment of the descending thoracic aorta: diameter 28 mm, GCS=3%.

modeling in AS of various grades, but they are expensive and not very accessible.

At the same time, transthoracic echocardiography with a set of new diagnostic options, despite its technical and visualization shortcomings, still remains the method of choice for assessing the structure and function of the AV, left ventricular (LV) dysfunction, and the determination of the AS severity due to its high availability and low cost [4, 5, 7, 8, 13, 14]. Multiplanar transesophageal echocardiography (TEE) has significantly greater diagnostic capabilities in assessing the ultrasound anatomy and dysfunction of the AV and TA in AS [4, 5, 7, 8, 13, 14].

In recent years, the interest in assessing the TA wall biomechanics has increased due to the implementation of 2D speckle-tracking TEE technology, which allows calculating the circumferential strain (deformation along the circumference) of tissues with tubular structure [14-20]. Our previous studies have shown the high diagnostic value of this technique in assessing characteristics of the TA wall deformation in atherosclerosis of various grades [15], dilation and aneurysm of the ascending aorta [16, 17]. To assess the global deformation along the TA circumference, an ultrasound model for measuring the LV myocardial circumferential and radial strain along the short axis was extrapolated, which is well studied and has been used in clinical practice for a long time [21]. In addition, an experimental study by J. Petrini et al. [22] provided convincing data on the high accuracy of 2D speckle-tracking TEE in the quantitative assessment of TA wall deformation characteristics compared to sonomicrometry.

In summary, we hypothesized that 2D speckle-tracking TEE can be used to assess disorders of the TA wall

ISSN 0022-9040. Kardiologiia. 2025;65(7). DOI: 10.18087/cardio.2025.7.n2882

biomechanics in patients with AS. We believe that this study will determine the diagnostic value of aortic wall deformation indices as an available additional criterion for assessing the degree of TA remodeling and mechanical dysfunction in patients with AS of various grades at the stage of preoperative evaluation.

Aim

The aim of the study was to analyze disorders of the TA biomechanics in AS using segmental ultrasound assessment of aortic wall deformation characteristics and its relationship with parameters of transaortic hemodynamics.

Material and methods

The study included 120 people (60 men and 60 women). Group 1 consisted of 11 healthy volunteers represented by men (mean age 39 [37; 47] years), in whom the examination revealed no pathology of the AV and TA, and risk factors or signs of other cardiovascular diseases; Group 2 consisted of 109 patients with severe (n=76) and very severe (n=33) AS (mean age 69 [64; 73] years). The clinical characteristics of the patients are presented in Table 1. According to current guidelines, AS is considered severe if the values of the mean transaortic pressure gradient, Doppler-calculated area and aortic orifice area index are ≥40 mm Hg, ≤1 cm^2, and ≤0.6 cm^2/m^2, respectively, and very severe with ≥60 mm Hg, <0.6 cm^2, and <0.4 cm^2/m^2, respectively [4, 5, 8]. Group 2 was divided into subgroups, 2a that included patients with AS of bicuspid AV (n=47) and 2b that included patients with AS of tricuspid AV (n=62).

The study was performed in consistency with the standards of Good Clinical Practice and the principles of the Declaration of Helsinki, and approved by the Biomedical Ethics Committee (Protocol # 213, 12.05.2021). All patients and healthy volunteers gave their written informed consent to participate in the study. Exclusion criteria were absolute contraindications to TEE, atrial fibrillation, frequent extrasystole, aortic regurgitation of >grade 2, cardiomyopathy, LV ejection fraction <50%, and patient refusal to participate in the study.

Multiplanar 2D TEE was performed in fasting condition using an expert-class ultrasound diagnostic system Epiq 7G (Philips) with a X8-2t matrix transesophageal transducer. Esophageal intubation was performed with the patient lying on the left side after local anesthesia of the oropharyngeal mucosa (10% lidocaine spray). The ascending segment, the arch areas accessible for location, and the entire TA descending segment were visualized in longitudinal and cross sections

Table 1. Clinical characteristics of study patients (group 2)

Parameter	Value
Sample size, n	109
Men, n (%)	49 (44.9)
Women, n (%)	60 (55.1)
Age, years	69 [64; 73]
Degenerative aortic valve stenosis, n (%)	109 (100)
Ischemic heart disease, n (%)	52 (47.7)
Postinfarction cardiosclerosis, n (%)	14 (12.8)
History of coronary stenting, n (%)	23 (21.1)
Arterial hypertension, n (%)	98 (89.9)
History of stroke or transient ischemic attack, n (%)	6 (5.5)
Chronic kidney disease, stages 3-5 (creatinine clearance <60 ml/min/m^2), n (%)	7 (6.4)
Obesity (BMI ≥30 kg/m^2), n (%)	63 (57.8)
Type 2 diabetes mellitus or impaired glucose tolerance, n (%)	36 (33.1)
Smoking, n (%)	36 (33.1)
Dyslipidemia, n (%)	95 (87.2)
Dilatation of the ascending aorta (diameter >40 mm), n (%)	15 (13.7)
Dilatation of the descending aorta (diameter >26 mm), n (%)	15 (13.7)
Aortic valve:	
bicuspid, n (%)	47 (43.2)
tricuspid, n (%)	62 (56.8)
Transaortic pressure gradient: peak, mm Hg mean, mm Hg	87 [75; 104] 50 [44; 62]
Planimetric area of the aortic orifice, cm^2	0.71 [0.61; 0.85]
Doppler-echocardiography of the aortic orifice area, cm^2	0.62 [0.52; 0.8]
Doppler-echocardiographic index of the aortic orifice area, cm^2/m^2	0.34 [0.29; 0.41]
Aortic regurgitation:	
grade 0, n (%)	22 (20.2)
grade 1, n (%)	45 (41.3)
grade 2, n (%)	42 (38.5)
Atherosclerosis of the descending thoracic aorta:	
plaques <3 mm, n (%)	72 (66.1)
plaques >3 mm, n (%)	37 (33.9)
Carotid stenosis <50%, n (%)	101 (92.6)
Carotid stenosis ≥50%, n (%)	12 (11)
Femoral artery stenosis <50%, n (%)	80 (73.4)
Femoral artery stenosis ≥50%, n (%)	6 (5.5)
Left ventricular ejection fraction, %	67 [63; 70]
Left ventricular hypertrophy, n (%)	108 (99.1)
Left ventricular global longitudinal strain, %	-14.9 [-12.7; -17.9]
Treatment:	
• ASA, n (%)	76 (69.7)
• anticoagulants, n (%)	53 (48.6)
• lipid-lowering therapy, n (%)	94 (86.2)
• beta-blockers, n (%)	90 (82.5)
• nitrates, n (%)	3 (2.7)
• calcium antagonists, n (%)	4 (31.2)
• ACE inhibitors or ARB, n (%)	61 (55.9)
• aldosterone receptor antagonists, n (%)	40 (36.7)

BMI, body mass index; ASA, acetylsalicylic acid; ACE, angiotensin-converting enzyme; ARB, angiotensin II receptor blocker. Data are presented as the median and interquartile range (Me [Q1;Q3]); n (%), number of patients

according to the standard protocol, using xPlane scanning technology [8, 13, 14]. The anatomical structure of the AV, the degree of aortic regurgitation, the area and the aortic orifice area index were assessed. Blood flow in the LV outflow tract was recorded in the pulsed-wave Doppler mode. The procedure was recorded as a series of video clips on the device hard drive with subsequent off-line processing on a QLab workstation, version 15.5 (Philips). During the procedure, the electrocardiogram was synchronously recorded in the II modified lead, and systolic blood pressure (SBP, mmHg) and diastolic blood pressure (DBP, mmHg) were measured oscillometrically on the right shoulder with an automatic sphygmomanometer M2 Basic (Omron). Pulse blood pressure (PBP, mmHg) was calculated as PBP = SBP-DBP.

For 2D speckle-tracking studies, clear gray-scale transversal TA sections were obtained at the level of the sinuses of Valsalva, sinotubular junction, bifurcation of the pulmonary artery; also, a transverse section of the descending TA was obtained at a standard point at a depth of 25-30 cm from the incisors. All ultrasound sections of the TA were obtained at the optimal frame rate (55-60 Hz), had clear contours of the intima-media complex and adventitia, and were recorded outside the zone of atherosclerotic plaques.

The TA diameter (mm) was measured at the level of the aortic annulus, sinuses of Valsalva, sinotubular junction, pulmonary artery bifurcation, and descending aorta in the proximal segment, which was indexed to the body surface area. The global peak systolic circumferential Lagrangian strain (GCS, %) was calculated in the ascending aorta at the level of the sinuses of Valsalva, sinotubular junction, pulmonary artery bifurcation, and in the proximal segment of the descending aorta, using a validated model for the LV in the short axis (see Central Illustration). In this case, the most accurate tracing of the inner contour of the zone of interest was performed along the surface of the intima-media complex, and of the outer contour along the outer border of the adventitia. According to this model, the aortic cross-section was divided into 6 conditional segments, in each of which the software module calculated the local strain with subsequent summation and provision of the global strain value over the entire circumference. The Doppler-calculated time of AV closure based on the blood flow spectrum in the LV outflow tract was set in the program manually. The software automatically calculated the time of reaching the peak systolic circumferential strain (time to peak, TTP, ms) and the change in the aortic cross-sectional area (fraction area change, FAC, %) during the cardiac cycle. Then, the global peak systolic circumferential Lagrangian strain normalized to PAP (GCS/PAP·100) and the β2 aortic wall stiffness index proposed by Y. Oishi et al. [23] were calculated using the formula:

$$\ln (SBP/DBP)/GCS \times 100.$$

Statistical analysis was performed using the STATISTICA software package, version 10.0 (StatSoft Inc.). The type of sample distribution was determined with the Shapiro-Wilk test. Given the absence of a normal sample distribution, the data were presented as a median and quartiles (Me [Q1; Q3]). Intergroup differences were assessed using the Mann-Whitney U-test. The relationship of the peak and mean transaortic pressure gradients with the aortic wall global circumferential strain was assessed with the Spearman correlation coefficients. Differences were considered statistically significant at $p<0.05$.

Results

In healthy volunteers (group 1), no AV pathology or deviations from normal values of TA sizes were detected along the entire length. A unidirectional, uniform circumferential aortic wall strain was observed in all segments averaging 9.7% [8.4; 11.7] and 18.4 [14.9; 20.6] with normalization of the indicator to the PBP value (Table 2). Also, healthy individuals had a uniform change in the cross-sectional area of all TA segments throughout the cardiac cycle and a significantly lower aortic wall stiffness index compared to AS patients (group 2). The peak and mean transaortic pressure gradients in healthy individuals were 8 [7; 10] mm Hg and 4 [4; 5] mm Hg, respectively.

In patients with AS, the values of aortic wall strain (GCS, GCS/PAD) and changes in the cross-sectional area in all TA segments were significantly lower than in healthy volunteers (Table 2).

Furthermore, in patients with AS, the aortic wall stiffness, as well as the diameter of the TA ascending and descending segments were significantly increased. Similar trends were observed for the intergroup comparisons of the mean TA diameter, aortic wall strain parameters, its stiffness, and changes in the cross-sectional area in all TA segments. Intragroup analysis revealed a negative aortic wall strain in 27 (24.7%) AS patients in the sinuses of Valsalva, in 16 (14.7%) in the sinotubular junction, and in 26 (23.2%) in the ascending aorta (see Central Illustration). Thus, 69 (63.3%) patients with AS had multidirectional circumferential aortic wall strain in the aortic root, ascending and descending segments of the TA. It should be noted that

ISSN 0022-9040. Kardiologiia. 2025;65(7). DOI: 10.18087/cardio.2025.7.n2882

Table 2. Values of systemic arterial pressure, morphometry, deformation and stiffness of the thoracic aorta in healthy individuals and patients with degenerative aortic valve stenosis by transesophageal echocardiography

Ultrasonic sections of the thoracic aorta		Group 1 (n=11)	Group 2 (n=109)	p_{1-2}	Subgroup 2a (n=47)	Subgroup 2b (n=62)	p_{2a-2b}
Aortic valve annulus	Diameter, mm	20 [19; 21]	20 [20; 22]	0.32	21 [20; 23]	20 [20; 22]	<0.05
Sinuses of Valsalva	Diameter, mm	32 [29; 36]	31 [29; 34]	0.51	31 [29; 36]	30 [29; 33]	<0.01
	GCS, %	12.2 [9.9; 13.4]	3.1 [1.3; 4.4]	<0.001	2.7 [-2.8; 4.4]	3.2 [2.2; 4.5]	0.29
	GCS/PBP	20.2 [17; 28.6]	3.8 [1.5; 5.9]	<0.001	3.8 [-3.5; 7.1]	3.8 [2.2; 5.3]	0.96
	FAC, %	24.3 [17.9; 27.6]	10.4 [7.3; 13.5]	<0.001	10.2 [7.2; 13.5]	10.8 [7.6; 13.7]	0.91
	TTP, ms	125.7 [80.6; 202.3]	129 [103.5; 168.2]	0.92	126.1 [99.3; 171]	137.7 [107.3; 168.2]	0.37
	β_2 stiffness index by Oishi Y. et al.	4.8 [3.6; 5.3]	19.1 [12.9; 26.5]	<0.001	18.3 [10.6; 23.7]	19.3 [15.3; 26.8]	0.22
Sinotubular junction	Diameter, mm	29 [26; 30]	30 [28; 32]	0.18	31 [28; 34]	29 [26; 31]	<0.01
	GCS, %	8.4 [5.6; 10]	4.5 [2.4; 6.5]	<0.001	4.8 [2.1; 6.5]	4.5 [2.5; 6.4]	0.85
	GCS/PBP	14.7 [10.9; 18.6]	5.7 [3.3; 8.7]	<0.001	7.4 [3.7; 10.2]	5 [3.2; 7.7]	0.05
	FAC, %	20.1 [13.1; 22.5]	10.3 [5.5; 14.2]	<0.001	10.6 [5.2; 14.5]	10.1 [5.5; 13.8]	0.97
	TTP, ms	119.4 [74.9; 214.3]	124.7 [78.7; 169]	0.44	139.5 [78.8; 175]	121.9 [78; 163.8]	0.57
	β_2 stiffness index by Oishi Y. et al.	6.7 [5.6; 8.3]	13.4 [10.1; 19.9]	<0.001	12.1 [8.6; 18.3]	14.6 [11.2; 20.5]	0.09
Ascending segment (level of pulmonary artery bifurcation)	Diameter, mm	29 [28; 33]	35 [32; 38]	<0.01	37 [34; 41]	34 [31; 36]	<0.001
	GCS, %	8.6 [7.6; 11.7]	3.1 [0.8; 4.7]	<0.001	2.9 [1.6; 4.6]	3.2 [–0.6; 5.3]	0.61
	GCS/PBP	18.0 [12.1; 20.2]	3.9 [1.4; 6.4]	<0.001	4.3 [1.6; 6.6]	3.8 [–0.8; 6.4]	0.46
	FAC, %	17.7 [16; 22.6]	7.9 [4.4; 11.6]	<0.001	7.8 [4.4; 10.5]	8.2 [4.1; 13.8]	0.29
	TTP, ms	96.1 [69.7; 154.9]	125 [88.1; 163.6]	0.23	114.9 [81.9; 155.3]	133.6 [89.4; 176.8]	0.21
	β2 stiffness index by Oishi Y. et al.	5.6 [4.6; 8.1]	17.8 [13.4; 26.9]	<0.001	18.2 [13.5; 24.1]	17.8 [13.4; 26.9]	0.99
Descending segment	Diameter, mm	22 [21; 23]	24 [22; 25]	<0.01	24 [23; 26]	24 [22; 25]	0.23
	GCS, %	10.4 [7; 11.2]	3.9 [3.1; 6]	<0.001	4.7 [3.5; 6.5]	3.5 [2.7; 5]	<0.01
	GCS/PBP	17.2 [14.1; 21.5]	5.6 [3.6; 8.4]	<0.001	7.5 [5; 10.4]	4.2 [3.2; 6.5]	<0.001
	FAC, %	17.5 [15; 21.5]	7 [0.9; 10.5]	<0.001	6.8 [0.8; 10.5]	7.2 [0.9; 10.7]	0.84
	TTP, ms	33.3 [24; 51.6]	73 [45.9; 110]	<0.01	64.2 [40.2; 98]	78.7 [47; 121.9]	0.09
	β2 stiffness index by Oishi Y. et al.	5.6 [4.6; 7.4]	17.2 [11.1; 25.3]	<0.001	11.5 [9.4; 19.3]	20.4 [14.2; 28.1]	<0.001
Averaged values for all thoracic aorta segments	Diameter, mm	26.6 [25.2; 28.4]	28 [26.6; 29.8]	<0.05	29.2 [27.4; 31.4]	27.4 [26; 28.8]	<0.001
	GCS, %	9.7 [8.4; 11.7]	3.3 [2.1; 4.4]	<0.001	3.5 [2.2; 4.3]	3.2 [1.8; 4.5]	0.84
	GCS/PBP	18.4 [14.9; 20.6]	4.6 [2.6; 6.5]	<0.001	5.1 [2.8; 7.6]	3.9 [2.1; 6.1]	0.07
	FAC, %	18.8 [17.6; 22.3]	8.4 [7; 11]	<0.001	8.4 [7.2; 10.5]	8.5 [6.8; 11.3]	0.71
	TTP, ms	114.6 [82.7; 137.2]	116.2 [93.9; 136.9]	0.45	111.2 [92.1; 135]	120.1 [93.9; 139.5]	0.25
	β_2 stiffness index by Oishi Y. et al.	5.9 [4.8; 6.7]	14.4 [7.6; 20.9]	<0.001	12.6 [6.4; 17.6]	15.6 [8.2; 22.1]	0.17
SBP, mm Hg		137 [125; 143]	149 [137; 171]	<0.01	142 [129; 158]	158 [141; 172]	<0.01
DBP, mm Hg		75 [74; 84]	75 [69; 81]	0.34	76 [73; 83]	72.5 [68; 80]	0.09
PBP, mm Hg		59 [50; 65]	76 [61; 91]	<0.01	64 [52; 82]	83.5 [69; 98]	<0.001
HR, beats/min		64 [54; 67]	69 [61; 76]	0.06	71 [61; 76]	68.5 [61; 78]	0.67

GCS, global circumferential strain; FAC, aortic fraction area change; TTP, time to peak systolic circumferential strain; SBP, systolic blood pressure; DBP, diastolic blood pressure; PBP, pulse blood pressure; HR, heart rate. Data are presented as the median and interquartile range (Me [Q1;Q3]).

despite the multidirectional strain in adjacent TA segments, the total AS patient group demonstrated a uniform decrease in the characteristics of aortic wall strain and an increase in its stiffness in all TA segments from the aortic annulus to the descending section (Table 2). No statistically significant difference was found between the strain and stiffness indices of the aortic wall in all TA segments between AS patients with bicuspid AV (subgroup 2a) and tricuspid AV (subgroup 2b) (see Table 2). At the same time, the diameter of the aortic root and ascending section in patients with AS in subgroup 2a was statistically significantly greater than in subgroup 2b with AS. No intergroup differences were found in the time to peak (TTP) systolic circumferential strain.

A statistically significant inverse correlation was found between the peak transaortic pressure gradient and GCS, GCS/PAP at the level of the sinuses of Valsalva ($r= -0.29$; $p<0.01$ and $r=-0.22$; $p<0.05$, respectively), and at the level of the ascending aorta ($r=-0.24$; $p<0.05$ and $r=-0.21$; $p<0.05$, respectively), as well as between the mean transaortic pressure gradient and GCS, GCS/PAP at the level of the sinuses of Valsalva ($r=-0.33$; $p<0.01$ and $r=-0.26$; $p<0.01$, respectively), and at the level of the ascending aorta ($r=-0.23$; $p<0.05$ and $r=-0.21$; $p<0.05$, respectively).

Discussion

Magnetic resonance imaging with a 4D Flow option (4D Flow MRI) is currently the most informative diagnostic tool in the preoperative evaluation of patients with severe AS, allowing for a comprehensive assessment of various variants of structural and functional disorders of the AV, LV, transaortic hemodynamics, and TA remodeling [7-12]. At the same time, these studies are expensive, inaccessible and therefore remain the prerogative of mainly large medical centers. In this regard, transthoracic and transesophageal echocardiography, despite certain technical and visualization limitations, still remain the leading methods of diagnosis and assessment of the severity of AS and its complications, being inexpensive and accessible [7, 8].

In recent years, using new tomographic techniques with 3D reconstruction, it has been found that in severe AS, due to structural changes in the AV and pronounced narrowing of the aortic orifice, there is not only an increase in the transaortic pressure gradient, but also the occurrence of high-speed turbulent vortex and spiral blood flows in the TA, primarily in the ascending aorta, displacement and loss of kinetic energy of the blood flow, as well as a disproportionate increase in the aortic wall shear stress during the cardiac cycle [9-12]. All these changes are accompanied by disorders of the normal aortic wall biomechanics and lead to gradual maladaptive TA remodeling with the formation of various phenotypes of aortopathy: dilation, aneurysm or dissection [9-12]. Thus, studying disorders of the aortic wall biomechanics and the degree of aortic remodeling in severe AS is an important addition to ultrasound biometry of the TA and the assessment of transaortic hemodynamics and aortic orifice area in the preoperative examination algorithm in this category of patients.

In this regard, of interest is the ultrasound examination of the TA biomechanics using 2D speckle-tracking TEE technology that allows calculating the aortic wall circumferential strain, an integral indicator reflecting the strain characteristics in the area of interest along the entire aortic circumference [14-20]. The advantage of this method is the superposition of 2D speckle-tracking technology on high-resolution gray-scale transverse ultrasound sections of the TA obtained with a high-frequency matrix transesophageal sensor located near the area of interest. The method is based on extrapolation of the ultrasound model for assessing the LV myocardium circumferential and radial strain, which is widely used in clinical practice and validated under experimental conditions on an aortic phantom [22].

We performed transesophageal ultrasound study of the TA biomechanics in patients with severe AS using segmental assessment of the aortic wall strain characteristics and assessed the relationship of aortic wall disorders with parameters of transaortic hemodynamics. In healthy volunteers without structural and functional disorders of the AV, with laminar transaortic blood flow and normal TA sizes throughout the cardiac cycle, we observed a uniform unidirectional deformation and uniform stiffness of the aortic wall in all studied TA segments in the direction from the AV annulus to the descending aorta. In our opinion, this is due to the adequate functioning of the unchanged tricuspid AV and the work of the elastic aortic compression chamber, which acts as a pulse wave damper. 4D Flow MRI of the TA in healthy volunteers confirmed the central laminar transaortic blood flow in the ascending aorta without loss of its kinetic energy and axial displacements, the absence of vortex and spiral turbulent blood flows and proportional shear stress of the TA wall during the cardiac cycle [9]. This, in turn, ensures a balanced transition of the blood flow kinetic energy into the potential energy of aortic wall deformation, which in healthy individuals, has a uniform and unidirectional character.

ISSN 0022-9040. Kardiologiia. 2025;65(7). DOI: 10.18087/cardio.2025.7.n2882

In patients with AS, we observed a statistically significant increase in the diameter of the TA ascending and descending sections, a uniform decrease in the deformation characteristics of the aortic wall, including to negative values, and an increase in its stiffness in all TA segments from the AV annulus to the descending section when compared with the group of healthy volunteers. Furthermore, the inverse correlation we identified between the parameters of transaortic hemodynamics and the aortic wall deformation indicates a relationship between the increase in the peak and average pressure gradients of turbulent blood flows through the narrowed aortic orifice with increasing severity of AS, calculated by dopplerography using the flow continuity equation, and a proportional decrease in the deformation characteristics of the root wall and the ascending aorta, calculated using the circumferential strain values. According to the Bernoulli theorem and Laplace's law [24], a decrease in deformation characteristics and an increase in the aortic wall strain create conditions for its gradual remodeling, leading to passive expansion of the TA in patients with severe AS, which was confirmed in this study. Also, an additional factor contributing to the mechanical dysfunction of the aortic wall and its maladaptive remodeling is the aortic wall multidirectional circumferential strain in the aortic root and the ascending and descending TA, which we identified in 69 (63.3%) patients with AS. 4D Flow MRI showed that deformation shifts of the aortic wall with opposite values within one segment or adjacent segments of the TA, caused by different velocities of local vortex turbulent blood flow and lateral pressure values, as well as blood flow shear in the aortic lumen, predict rapid passive expansion and dissection [9]. Furthermore, the most pronounced changes described above were detected in patients with bicuspid AV stenosis [9-12]. At the same time, we did not find a statistically significant difference between the deformation and stiffness parameters of the aortic wall in any TA segments between AS patients with bicuspid AV and tricuspid AV. Apparently, at the stages of severe and very severe AS, when we detect pronounced calcification of the AV cusps, critical narrowing of the aortic orifice, and impaired transaortic hemodynamics, the anatomical variant of the AV structure no longer affects the indices of mechanical dysfunction of the aortic wall. At the same time, the final remodeling of the root and ascending aorta evident as an increased diameter in AS patients with bicuspid AV, according to our data, was more pronounced than in AS patients with tricuspid AV. The non-informativity of the TTP systolic circumferential strain, in our opinion, is due to the participation of patients with multidirectional deformation of the aortic wall within one TA ultrasonic segment.

Thus, a comprehensive ultrasound assessment of the AV anatomy, transaortic hemodynamic, morphometry, and biomechanics of the TA can be used in the preoperative examination algorithm in patients with severe and very severe AS as an accessible non-invasive diagnostic tool for determining the degree of AV dysfunction, remodeling and mechanical dysfunction of the TA wall at different levels.

Study limitations

This study had certain limitations. We had to exclude from the study individuals whose transverse ultrasound section of the descending TA at the optimal frame rate (53-60 Hz) went beyond the specified sector of the grayscale image, which did not allow the software to accurately trace the intimal and adventitial contours of the aortic wall around the circumference. In addition, we did not include individuals with limitations in ultrasound visualization of the ascending aorta transverse sections due to air shielding in the trachea and the left main bronchus.

Conclusions

The TA circumferential strain is a new quantitative ultrasound marker of mechanical dysfunction and remodeling of the aortic wall in AS. Severe AS is associated with uniform decreases in deformation characteristics of the aortic wall down to negative values and an increased stiffness in all TA segments from the AV annulus to the descending section, closely associated with impaired transaortic hemodynamics. Patients with severe AS have maladaptive remodeling and multidirectional deformation along the circumference of the aortic wall in the aortic root, and the the ascending and descending TA. In severe AS of both bicuspid and tricuspid AVs, despite different degrees of aortic wall remodeling, the deformation and stiffness parameters in all TA segments do not differ significantly.

Comprehensive ultrasound assessment of the AV anatomy, parameters of transaortic hemodynamics, and the TA morphometry and biomechanics is a highly informative diagnostic tool for determining the degree of AV dysfunction and the TA wall remodeling and dysfunction at different levels in patients with severe AS at the stage of preoperative examination.

Funding

The study was performed at the Research Institute of Cardiology of the Tomsk National Research Medical Center of the Russian Academy of Sciences as part of the state

assignment on "Fundamental aspects of the formation of structural and functional changes in the heart and blood vessels in different age groups at the preclinical, clinical stages, and after hemodynamic correction of cardiovascular diseases", registration number 122020300044-8 in the Unified State Information System for Registration and Accounting of Scientific, Research, and Experimental Design Works.

No conflict of interest was declared.

The article was received on 27/01/2025

REFERENCES

1. Lindman BR, Sukul D, Dweck MR, Madhavan MV, Arsenault BJ, Coylewright M et al. Evaluating Medical Therapy for Calcific Aortic Stenosis: JACC State-of-the-Art Review. Journal of the American College of Cardiology. 2021;78(23):2354–76. DOI: 10.1016/j.jacc.2021.09.1367
2. Zebhi B, Lazkani M, Bark D. Calcific Aortic Stenosis – A Review on Acquired Mechanisms of the Disease and Treatments. Frontiers in Cardiovascular Medicine. 2021;8:734175. DOI: 10.3389/fcvm.2021.734175
3. Dahou A, Awasthi V, Bkhache M, Djellal M, Yang X, Wang H et al. Sex-Related Differences in the Pathophysiology, Cardiac Imaging, and Clinical Outcomes of Aortic Stenosis: A Narrative Review. Journal of Clinical Medicine. 2024;13(21):6359. DOI: 10.3390/jcm13216359
4. Vahanian A, Beyersdorf F, Praz F, Milojevic M, Baldus S, Bauersachs J et al. 2021 ESC/EACTS Guidelines for the management of valvular heart disease. European Heart Journal. 2022;43(7):561–632. DOI: 10.1093/eurheartj/ehab395
5. Otto CM, Nishimura RA, Bonow RO, Carabello BA, Erwin JP, Gentile F et al. 2020 ACC/AHA Guideline for the Management of Patients With Valvular Heart Disease: Executive Summary: A Report of the American College of Cardiology/American Heart Association Joint Committee on Clinical Practice Guidelines. Circulation. 2021;143(5):e35–71. DOI: 10.1161/CIR.0000000000000932
6. Ergashev Sh.S., Petlin K.A., Kozlov B.N., Alyamkin V.E., Chernykh Yu.N. Mid-term hemodynamic results of bioprosthetics of the aortic valve with a prosthesis with a unique "easy change" system. Siberian Journal of Clinical and Experimental Medicine. 2024;39(2):86–93. [Russian: Эргашев Ш.С., Петлин К.А., Козлов Б.Н., Алямкин В.Е., Черных Ю.Н. Среднесрочные гемодинамические результаты биопротезирования аортального клапана протезом с уникальной системой «easy change». Сибирский журнал клинической и экспериментальной медицины. 2024;39(2):86–93]. DOI: 10.29001/2073-8552-2024-39-2-86-93
7. Cionca C, Zlibut A, Agoston-Coldea L, Mocan T. Advanced cardiovascular multimodal imaging and aortic stenosis. Heart Failure Reviews. 2022;27(2):677–96. DOI: 10.1007/s10741-021-10131-8
8. Dweck MR, Loganath K, Bing R, Treibel TA, McCann GP, Newby DE et al. Multi-modality imaging in aortic stenosis: an EACVI clinical consensus document. European Heart Journal – Cardiovascular Imaging. 2023;24(11):1430–43. DOI: 10.1093/ehjci/jead153
9. Garcia J, Barker AJ, Markl M. The Role of Imaging of Flow Patterns by 4D Flow MRI in Aortic Stenosis. JACC: Cardiovascular Imaging. 2019;12(2):252–66. DOI: 10.1016/j.jcmg.2018.10.034
10. Fatehi Hassanabad A, King MA, Di Martino E, Fedak PWM, Garcia J. Clinical implications of the biomechanics of bicuspid aortic valve and bicuspid aortopathy. Frontiers in Cardiovascular Medicine. 2022;9:922353. DOI: 10.3389/fcvm.2022.922353
11. Emendi M, Sturla F, Ghosh RP, Bianchi M, Piatti F, Pluchinotta FR et al. Patient-Specific Bicuspid Aortic Valve Biomechanics: A Magnetic Resonance Imaging Integrated Fluid–Structure Interaction Approach. Annals of Biomedical Engineering. 2021;49(2):627–41. DOI: 10.1007/s10439-020-02571-4
12. Qin JJ, Obeidy P, Gok M, Gholipour A, Grieve SM. 4D-flow MRI derived wall shear stress for the risk stratification of bicuspid aortic valve aortopathy: A systematic review. Frontiers in Cardiovascular Medicine. 2023;9:1075833. DOI: 10.3389/fcvm.2022.1075833
13. Evangelista A, Sitges M, Jondeau G, Nijveldt R, Pepi M, Cuellar H et al. Multimodality imaging in thoracic aortic diseases: a clinical consensus statement from the European Association of Cardiovascular Imaging and the European Society of Cardiology working group on aorta and peripheral vascular diseases. European Heart Journal – Cardiovascular Imaging. 2023;24(5):e65–85. DOI: 10.1093/ehjci/jead024
14. Isselbacher EM, Preventza O, Hamilton Black J, Augoustides JG, Beck AW, Bolen MA et al. 2022 ACC/AHA Guideline for the Diagnosis and Management of Aortic Disease: A Report of the American Heart Association/American College of Cardiology Joint Committee on Clinical Practice Guidelines. Circulation. 2022;146(24):e334–482. DOI: 10.1161/CIR.0000000000001106
15. Vrublevsky A.V., Boshchenko A.A., Bogdanov Yu.I., Saushkin V.V., Shnaider O.L. Structural and Functional Disturbances of the Thoracic Aorta in Atherosclerosis of Various Gradations. Kardiologiia. 2023;63(11):64–72. [Russian: Врублевский А.В., Бощенко А.А., Богданов Ю.И., Саушкин В.В., Шнайдер О.Л. Структурно-функциональные нарушения грудного отдела аорты при атеросклерозе различных градаций. Кардиология. 2023;63(11):64–72]. DOI: 10.18087/cardio.2023.11.n2315
16. Vrublevsky A.V., Panfilov D.S., Kozlov B.N., Saushkin V.V., Sazonova S.I. Disturbances of the ascending aorta biomechanics in moderate dilatation and aneurysm. Russian Journal of Cardiology. 2023;28(5):55–63. [Russian: Врублевский А.В., Панфилов Д.С., Козлов Б.Н., Саушкин В.В., Сазонова С.И. Нарушения биомеханики восходящего отдела аорты при пограничном расширении и аневризме. Российский кардиологический журнал. 2023;28(5):55-63]. DOI: 10.15829/1560-4071-2023-5365
17. Saushkin V.V., Panfilov D.S., Vrublevsky A.V., Sazonova S.I., Kozlov B.N. Role of imaging modalities in the choice of treatment strategy for mega aorta syndrome. Pirogov Russian Journal of Surgery. 2022;2:67–74. [Russian: Саушкин В.В., Панфилов Д.С., Врублевский А.В., Сазонова С.И., Козлов Б.Н. Роль лучевых методов диагностики в выборе тактики лечения синдрома мегааорты. Хирургия. Журнал им. Н. И. Пирогова. 2022;2:67–74]. DOI: 10.17116/hirurgia202202167
18. Emmott A, Alzahrani H, Alreshidan M, Therrien J, Leask RL, Lachapelle K. Transesophageal echocardiographic strain imaging predicts aortic biomechanics: Beyond diameter. The Journal of Thoracic and Cardiovascular Surgery. 2018;156(2):503-512.e1. DOI: 10.1016/j.jtcvs.2018.01.107
19. Alreshidan M, Shahmansouri N, Chung J, Lash V, Emmott A, Leask RL et al. Obtaining the biomechanical behavior of ascending aortic aneurysm via the use of novel speckle tracking echocardiography. The Journal of Thoracic and

ISSN 0022-9040. Kardiologiia. 2025;65(7). DOI: 10.18087/cardio.2025.7.n2882

Cardiovascular Surgery. 2017;153(4):781–8. DOI: 10.1016/j.jtcvs.2016.11.056
20. Rong LQ, Kim J, Gregory AJ. Speckle tracking echocardiography: imaging insights into the aorta. Current Opinion in Cardiology. 2020;35(2):116–22. DOI: 10.1097/HCO.0000000000000706
21. Cameli M, Mandoli GE, Sciaccaluga C, Mondillo S. More than 10 years of speckle tracking echocardiography: Still a novel technique or a definite tool for clinical practice? Echocardiography. 2019;36(5):958–70. DOI: 10.1111/echo.14339
22. Petrini J, Eriksson MJ, Caidahl K, Larsson M. Circumferential strain by velocity vector imaging and speckle-tracking echocardiography: validation against sonomicrometry in an aortic phantom. Clinical Physiology and Functional Imaging. 2018;38(2):269–77. DOI: 10.1111/cpf.12410
23. Oishi Y, Mizuguchi Y, Miyoshi H, Iuchi A, Nagase N, Oki T. A Novel Approach to Assess Aortic Stiffness Related to Changes in Aging Using a Two-Dimensional Strain Imaging. Echocardiography. 2008;25(9):941–5. DOI: 10.1111/j.1540-8175.2008.00725.x
24. Caro C, Pedley T, Schroter R, Seed W. The mechanics of the circulation. - M.: Mir; 1981. - 624p. [Russian: Каро К., Педли Т., Шротер Р., Сид У. Механика кровообращения. – М.: Мир; 1981. – 624с]